Ultrasound-Assisted Extraction of Patin Fish Oil: Optimization Using Response Surface Methodology – Box Behnken Design

Anggita Rosiana Putri[1,2*], Widiastuti Setyaningsih[3], Miguel Palma[4], Ceferino Carrera Fernandez[4], Abdul Rohman[5], Sugeng Riyanto[6], and Young Pyo Jang[7]

[1]*Department of Pharmacy, Faculty of Medicine, Universitas Brawijaya, Jl. Veteran, Malang 65145, Indonesia*

[2]*Drug Development and Analytical Methods Research Group, Faculty of Medicine, Universitas Brawijaya, Jl. Veteran, Malang 65145, Indonesia*

[3]*Department of Food and Agricultural Product Technology, Faculty of Agricultural Technology, Universitas Gadjah Mada, Jl. Flora No. 1, Yogyakarta 55281, Indonesia*

[4]*Department of Analytical Chemistry, Faculty of Sciences, University of Cadiz, Campus de Excelencia Internacional Agroalimentario (CeiA3), Campus del Rio San Pedro, 11510, Cadiz, Spain*

[5]*Department of Pharmaceutical Chemistry, Faculty of Pharmacy, Universitas Gadjah Mada, Yogyakarta 55281, Indonesia*

[6]*Pharmacy Study Program, Gunadarma University, Jl. Margonda Raya No. 100, Depok 16954, Indonesia*

[7]*Division of Pharmacognosy, College of Pharmacy, Kyung Hee University, Dongdaemun-Gu, Seoul 02447, Republic of Korea*

**** Corresponding author:***

tel: +62-85791687831
email: anggita.rosiana@ub.ac.id

Received: March 7, 2025
Accepted: June 16, 2025

DOI: 10.22146/ijc.105223

Abstract: *The oil extracted from* Pangasius micronemus*, commonly known as patin fish, is highly regarded for its omega-3 and omega-6 fatty acids content, which offer numerous health benefits. Producing high-quality patin fish oil (PFO) rich in these essential fatty acids requires an optimized extraction process. This study utilized ultrasound-assisted extraction (UAE) combined with response surface methodology – Box Behnken Design (RSM-BBD) to optimize the extraction of PFO. Five variables were examined: temperature (30–60 °C), solvent composition (*n*-hexane in isopropanol, 30–90%), amplitude (30–90%), solvent-to-sample ratio (10:1–20:1), and cycle duration (0.2–0.8 s^{-1}). The analysis identified solvent composition, amplitude, and solvent-to-sample ratio as significant factors influencing the response value ($p < 0.005$). Optimal UAE conditions were achieved at a temperature of 59 °C, solvent composition of 42%, amplitude of 41%, solvent-to-sample ratio of 20:1, cycle duration of 0.8 s^{-1}, and an extraction time of 25 min. Fatty acid profiling revealed that PFO extracted using UAE contained omega-3 fatty acids, including α-linolenic acid (ALA) at 1.36% and eicosapentaenoic acid (EPA) at 0.46%, as well as omega-6 fatty acids, namely linoleic acid (LA) at 19.06% and arachidonic acid (AA) at 0.85%. These results demonstrate the efficiency of UAE in extracting high-quality PFO.*

Keywords: *PFO; optimization; ultrasound-assisted extraction; response surface methodology; Box-Behnken design*

■ INTRODUCTION

Fish oil is known for its high nutritional value components such as omega-3 and omega-6 fatty acids, which are essential ingredients of the human diet and play important roles in maintaining health. Fish oil could be extracted from both marine and freshwater fish. However, the utilization of freshwater fish as a fish oil source is still limited, even though its nutritional value is comparable. One example of freshwater fish that could be promoted as a fish oil source is the patin fish

(*Pangasius micronemus*), which is widely cultivated and readily available in several regions in Indonesia.

The oil from patin fish or patin fish oil (PFO) was reported to contain essential fatty acids such as omega-3 [1]. Omega-3 is a polyunsaturated fatty acid (PUFAs) with more than one double bond carbon (C=C) functional group in its backbone [2]. These fatty acids include arachidonic acid (ARA), α-linolenic acid (ALA), eicosapentaenoic acid (EPA), and docosahexaenoic acid (DHA) [3]. Omega-3 fatty acid can help overcome some health problems, such as reducing inflammation and lowering the risk of chronic diseases such as heart disease, cancer, and arthritis. These fatty acids also regulate blood pressure, hematic clotting, glucose tolerance, and nervous system development and functions [4].

In order to obtain the fish oil from the patin fish, an extraction procedure needs to be done. Some common lipid extraction methods include Soxhlet and maceration techniques. However, several drawbacks from these methods, such as long-time processing that could take up to 24 h and require massive amounts of solvent, are serious issues for large-scale production. Therefore, some alternative methods have been proposed to overcome these problems. Extraction using ultrasound technology could reduce the extraction time and the solvent consumption [5].

Ultrasound-assisted extraction (UAE) is extensively utilized for extracting oils from diverse plant and microbial sources, owing to its effectiveness in improving mass transfer, decreasing extraction duration, and reducing solvent usage [5-10]. Multiple studies have documented the effective utilization of UAE in lipid extraction from flaxseed [5], fungi such as *Mortierella isabellina* [6], oleaginous seeds [7], and in the enhancement of quality indices in virgin avocado oil production [10]. Moreover, the UAE has been acknowledged as an environmentally friendly and sustainable method, as evidenced by extensive analyses of its processes and uses in the extraction of bioactive chemicals and natural products [8-9]. Despite its established benefits, the use of UAE for fish oil extraction is still quite limited. No research has been undertaken to optimize the UAE method for oil extraction from patin fish. This offers a significant opportunity to investigate the possibility of UAE as an innovative and effective method for extracting oil from patin fish.

Some reports confirmed that the UAE method results in higher extraction yield of various lipids at reduced extraction time and reduced solvent consumption [5-7]. When ultrasound is applied in the liquid medium, numerous bubbles will be produced. These bubbles will grow and oscillate quickly before collapsing due to pressure changes. These violent implosions will fragment or disrupt the surface of the solid matrix, cause the release of lipid in the solvent, enhancing mass transfer and accelerate the diffusion [8-9]. Tan et al. [10] reported that the application of UAE resulted in higher extraction yield and higher levels of unsaturated fatty acid.

Different processes that occur during cavitation (i.e., nucleation, bubble growth, and collapse) are affected by several factors. The initial step, including formation of the cavitation bubbles is one of the most important parameters. The increase of ultrasonic frequency could decrease the formation of bubbles due to insufficient time for the rarefaction cycle which allows the growth of the bubble, so that disruption of the liquid can be produced. The number of nuclei for cavitation depends on temperature. Other than that, the efficiency of the UAE is affected by solvent composition, the ratio of sample to solvent, and ultrasound power. As there are several factors affecting the extraction process, an optimization of the aforementioned factors needs to be employed in order to obtain the highest extraction yield [11-12].

A Box-Behnken design (BBD) is often used to investigate the interaction effects among several factors at the same time. This is succeeded by response surface methodology (RSM) to identify the optimal process conditions. As a result, this research aimed to establish a dependable extraction condition for PFO through ultrasound-assisted extraction, employing BBD alongside RSM. BBD serves as a highly effective statistical instrument that facilitates the organized exploration of the connections between independent variables, all while reducing the necessary number of experimental runs. This design is especially appropriate

for optimization studies as it circumvents extreme factor combinations that could result in unsatisfactory or unsafe experimental conditions [11].

The combination of RSM and BBD facilitates the creation of a second-order polynomial model capable of predicting responses throughout the design space. This study focused on three important variables: extraction time, temperature, and solvent-to-sample ratio, chosen for their anticipated impact on oil yield and quality. The experimental data gathered from the BBD were analyzed through ANOVA to evaluate the significance of each factor and their interactions [12]. Subsequently, response surface plots and contour diagrams were created to illustrate the optimal conditions. This method guarantees both the optimization of extraction efficiency and the establishment of a strong and consistent process for acquiring high-quality PFO.

■ EXPERIMENTAL SECTION

Materials

The chemicals used in the study included *n*-hexane with a purity of ≥ 97.0% (HPLC grade) from Riedel-de Haen, Germany; isopropanol (HPLC grade) from Labkem, Barcelona, Spain; and potassium hydroxide (KOH) along with methanol (HPLC grade) from Merck, Darmstadt, Germany.

Instrumentation

Ultrasound irradiation was applied using ultrasonic probe UP 200S (Hielscher Ultrasound Technology, Berlin, Germany) coupled with a thermostatic bath (Frigiterm-10, Selecta, Barcelona, Spain) to control the temperature, rotary evaporator (IKA-Werke GmbH & Co. Kg, Stauten, Germany), gas chromatography coupled with mass spectrometry (GC-MS) model TQ8040 (Shimadzu, Japan), and laboratory glasswares.

Procedure

Sample preparations

The UAE was conducted using an ultrasonic probe UP 200S, which allows control and modification of the cycle and amplitude. The system was coupled with a thermostatic bath to maintain the temperature. Precisely 1 g of fish powder was weighed and placed in an extraction tube, followed by the addition of 10 mL of a solvent mixture of *n*-hexane and isopropanol. The extraction procedure was performed according to the optimum conditions identified through RSM-BBD. After the extraction process, the solid material was separated by filtration, and the solvent was removed using a rotary evaporator at 40 °C.

BBD and statistical analysis

RSM was employed to optimize the extraction method. The experimental variables studied using a BBD included temperature (X_1), solvent composition (X_2), amplitude (X_3), solvent to sample ratio (X_4), and cycle (X_5), each at three levels (−1, 0, 1). The range of these variables is listed in Table 1, and the complete experimental design, consisting of 46 experiments, is detailed in Table 2. The percentage yield of PFO was used as the response variable. The yield of PFO was calculated in Eq. (1):

$$\text{Yield } (\%) = \frac{W_2}{W_1} \times 100\% \quad (1)$$

where W_2 is the mass of PFO extracted from the sample (g) and W_1 is the mass of the dried samples (g).

By fitting the data to a polynomial approach, the experiment design method was utilized to determine the surface response and assess the impacts of each variable as well as the interactions between them. After every variable is assessed, the RSM can be stated as shows in Eq. (2):

$$y = f(x_1, x_2, x_3, \cdots, x_k) \quad (2)$$

where y is the experimental design response and x is the set of factors or variables. It is assumed that the variables are continuous and controllable during the experiment. The ultimate goal was to maximize the response y, which required determining the best estimate for the correlation between factors and the response surface. Typically, a second-order model is used in RSM (Eq. (3)).

Table 1. The variables of the design of the experiment

Factors	Variables	−1	0	+1	Units
X_1	Temperature	30.0	45.0	60.0	°C
X_2	Solvent composition	30.0	60.0	90.0	%
X_3	Amplitude	30.0	60.0	90.0	%
X_4	Solvent to sample ratio	10.0	15.0	20.0	mL/g
X_5	Cycle	0.2	0.5	0.8	s^{-1}

Table 2. Box-Behnken design of design of experiment

Run	Temperature (°C)	Solvent composition (%)	Amplitude (A)	Sample to solvent ratio (w/v)	Cycle (s^{-1})	Yield (%)	Predicted (%)
1	1	0	0	0	−1	31.27	32.98
2	0	0	0	−1	−1	32.87	32.85
3	0	0	1	0	−1	30.47	29.79
4	0	0	0	0	0	34.49	34.95
5	0	0	0	0	0	34.34	34.95
6	0	0	−1	−1	0	34.86	34.11
7	0	0	0	0	0	34.72	34.95
8	0	−1	0	0	−1	34.86	33.51
9	0	0	−1	0	1	33.20	34.75
10	0	0	1	1	0	32.58	31.66
11	0	1	0	0	1	27.64	29.15
12	−1	0	0	1	0	31.48	32.08
13	0	1	0	0	−1	31.99	30.97
14	0	0	0	0	0	37.18	34.95
15	−1	0	0	0	−1	32.41	33.00
16	0	1	−1	0	0	33.09	33.58
17	1	0	0	−1	0	28.81	30.85
18	0	0	0	−1	1	32.53	31.76
19	0	0	0	0	0	33.29	34.95
20	0	−1	0	−1	0	33.57	32.14
21	−1	1	0	0	0	31.41	29.28
22	1	1	0	0	0	31.91	28.87
23	−1	0	−1	0	0	33.38	32.70
24	0	0	0	0	0	35.69	34.95
25	1	0	0	1	0	34.68	35.58
26	0	−1	0	0	1	34.16	35.34
27	0	−1	−1	0	0	34.21	33.85
28	1	0	1	0	0	29.17	29.03
29	0	1	1	0	0	22.56	24.53
30	−1	0	1	0	0	29.62	29.99
31	−1	−1	0	0	0	31.54	31.96
32	0	0	0	1	−1	35.31	34.26
33	0	1	0	−1	0	29.06	29.01
34	0	0	−1	0	−1	34.31	36.14
35	−1	0	0	0	1	32.63	31.71
36	0	0	1	−1	0	29.26	28.49
37	0	0	1	0	1	32.15	31.19
38	0	−1	1	0	0	31.86	32.99
39	0	0	−1	1	0	36.84	35.95
40	−1	0	0	−1	0	30.06	31.80
41	0	0	0	1	1	37.16	35.36
42	1	−1	0	0	0	35.41	34.92
43	0	1	0	1	0	28.00	30.28
44	1	0	−1	0	0	37.41	36.22
45	0	−1	0	1	0	34.99	35.88
46	1	0	0	0	1	34.07	34.28

$$y = \beta_0 + \sum_{1=1}^{k} \beta_i X_i + \sum_{1=1}^{k} \beta_{ii} X_{ii} + \sum_{1=1}^{k-1} \sum_{j=1}^{k} \beta_{ij} X_i X_j + \varepsilon \quad (3)$$

where X is the variable, β_{ii} (i = 1,2,…5), β_{ij} (i = 1,2,…5, j = 1,2,…5) are unknown parameters and ε is a random

error. The β is a coefficient obtained by the least squares regression method. The design of the experiment (DOE) matrix was obtained using STATGRAPHICS Centurion 18 (Statpoint Technologies, Inc., USA). To determine the significance of mean differences, ANOVA and least significant difference (LSD) were used.

Fatty acid analysis

The fatty acid content of PFO was analyzed using GC-MS. Prior to injection into the GC-MS instrument, the fatty acids were derivatized into their methyl ester form following a modified version of the procedure by Rohman et al. [13]. The derivatization process involved the use of sodium methoxide. To begin, 100 mg of oil was accurately weighed into a 10 mL centrifuge tube using an analytical balance, and 1.2 mL of *n*-hexane was added. The mixture was stirred using a vortex mixer for 1 min until the fat dissolved. Next, a 0.25 mL of 2 M methanolic potassium hydroxide solution was added, and the mixture was stirred for 5 min. The solution was then centrifuged for 5 min at 3000 rpm. Subsequently, 1–2 mL of the upper layer was transferred to a 2 mL vial, which was sealed with a silicone Teflon cap and septum for GC-MS analysis.

The fatty acids were analyzed by the GC-MS instrument using a BPX5 column (30 m × 0.25 μm × 0.25 μm). The GC temperature profile was initially started at 40 °C, held for 5 min at the rate of 3 °C/min to 200 °C, held for 5 min, and finally at the rate 40 °C/min held for 2 min. The carrier gas was helium, and the injection temperature was kept at 150 °C, while the column oven temperature set at 40 °C.

■ RESULTS AND DISCUSSION

Development of the UAE Method

An experimental design was made to evaluate the variables that influence the extraction yield. The variables consist of temperature (X_1; 30–60 °C), solvent composition (X_2; 30–90%), amplitude (X_3; 30–90%), solvent to sample ratio (X_4; 10:1–20:1), and cycle (X_5; 0.2–0.8 s^{-1}). The range of variables was chosen based on several previous studies on fatty acid extraction [14-15]. The response of an experimental design is expressed by %yield of fatty acid obtained from UAE extraction. The variables are shown in Table 1.

A BBD with 46 runs that included six center points were obtained by a mathematical model from STATGRAPHIC. ANOVA was applied to the set of results in order to evaluate the effect of the different factors on their response and the possible interactions between them. Table 2 shows the results obtained from this analysis. Pareto chart, as Fig. 1, explained the standardized effect ($p = 0.05$) in decreasing order of importance. A bar that crosses a vertical line shows the factor that has a significant effect on the response. According to the Pareto chart, several variables exhibit significant effects, including amplitude, solvent composition, solvent to sample ratio, the quadratic effects of solvent composition and amplitude, temperature, and the interaction between solvent composition and amplitude.

Based on the pareto chart in Fig. 1, the temperature (X_1), solvent to sample ratio (X_4), and cycle (X_5) give a

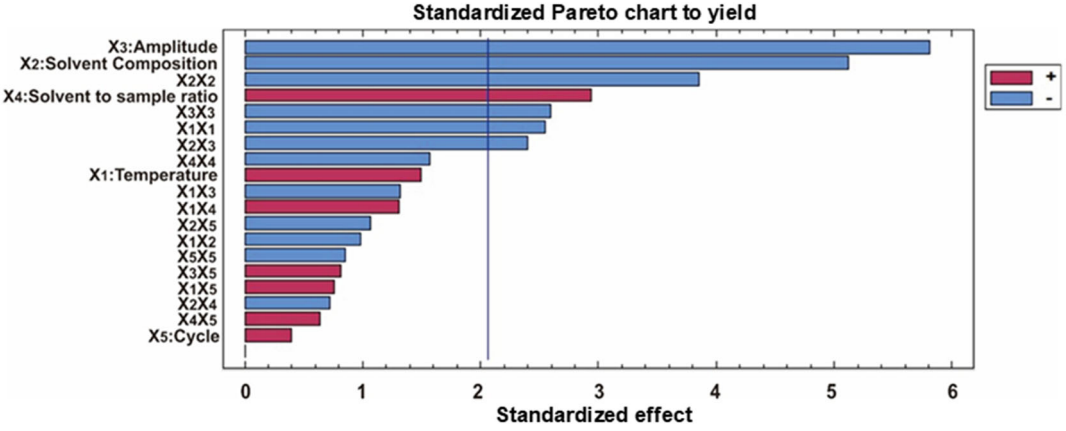

Fig 1. Pareto chart for standardized effect in decreasing order of importance

positive effect to the extraction yield. The positive effect means that increasing this factor increases the extraction yield [11]. An increase in temperature generally leads to a higher extraction yield within a specific time frame, as the extraction rate of most compounds tends to rise with temperature [9]. However, once the optimal extraction temperature has been reached, any further increase in temperature may lead to a decrease in the extraction yield. An increase in temperature can enhance vapor pressure, which influences the intensity of acoustic cavitation. Ultrasound generates fewer bubbles at lower temperatures; however, these bubbles collapse with greater force due to the higher pressure difference across the bubble interface, resulting from lower vapor pressure. Consequently, cell tissue disruption becomes more effective. Conversely, at higher temperatures, the pressure difference between the interior and exterior of the bubbles is smaller, leading to weaker bubble collapse and reduced cell tissue destruction.

Additionally, the decrease in surface tension with increasing temperature may also contribute to the reduction in cavitation intensity. At higher temperatures, the solvent's surface tension decreases, which weakens bubble collapse and subsequently reduces mass transfer intensity. This phenomenon directly results from the relationship between surface tension and pressure difference across the interface, as described by the Young-Laplace equation. Another contributing factor could be the greater degradation of oil at elevated temperatures and the increased loss of solvent, which may alter the solvent to sample ratio. This condition could negatively impact the efficiency of the extraction process [9,16].

Higher extraction yield could be obtained by increasing the solvent to sample ratio. Mohammadpour et al. [17], in their research about the extraction of *Moringa peregrina* oil using the UAE method, also confirmed that the solvent to sample ratio has a significant effect on the extraction yield. Increasing the concentration gradient enhance the rate of mass transfer from the solid matrix to the solvent. However, at higher solvent to solid ratios, this effect diminishes because the primary limitation to mass transfer occurs within the solid matrix. Additionally, excess solvent in the system, which corresponds to a low solid concentration, may reduce cavitation phenomena due to fewer nucleation sites, potentially negatively impacting the oil yield [9].

Regarding the solvent composition, increasing the solvent composition means the concentration of *n*-hexane is higher than isopropanol, causing a reduction in extraction yield. The physical properties of the solvent have an impact on the cavitation process. Isopropanol has a vapor pressure of 43 mbar, a viscosity of 2.27 mPas, a density of 0.785 g/cm^3 and a surface tension of 21.7 mN/m at 25 °C while *n*-hexane has vapor pressure of 266 mbar, a viscosity of 0.31 mPa, a density of 0.664 g/cm^3 and a surface tension of 18.4 mN/m [18]. Vapor pressure and surface tension are the two key factors that impact the cavitation intensity. The cavitation intensity decreases as vapor pressure and surface tension increase. So, when the concentration of *n*-hexane is more than isopropanol, there is a possibility to reduce the cavitation intensity [18].

In terms the amplitude or ultrasonic power, the rise of the amplitude caused a reduction in the extraction yield. This trend also showed up in the previous work. The oil would be degraded due to the thermal reaction at high ultrasonic power levels. The higher ultrasound power would make the bubbles in the solvent expand more rapidly and would reduce the efficiency of the ultrasound energy, which travels through the medium as reported by Sun et al. [19]. The application of sonication cycles showed a positive influence on the extraction yield. However, this effect was not statistically significant. When the number of cycles was excessively high, a decrease in yield was observed, as reported in previous studies [12,20]. The possible reason is that the higher cycle may cause the negative chemical and physical effects of cavitation [20-22]. The negative effect is often due to the reactions of free radicals formed during the sonication with molecules in the medium, which accelerates the degradation process of fish oil [23-24]. The phenomenon has also been observed in a previously reported study. The peroxide value of extracted oil was increased significantly by the UAE method, which indicated that the primary oxidation of extracted oils was accelerated under ultrasound owing to

the effect of cavitation [24].

Nonetheless, all variables were used to predict the fitting properties of the model. The polynomial equation (Eq. (4)) for yield were obtained from the coefficients of the effect and interactions, as listed in Table 3. Therefore, two second-order mathematical models were obtained to predict the yield response value as a function of the independent variables. Then, the result will be compared with the actual value of the yield, as shown in Fig. 2. Based on the polynomial model of Eq. (4), certain variables appear to have a more substantial effect on the yield. The temperature (X_1) and solvent to sample ratio (X_4) show relatively large positive coefficients, indicating that increases in these variables may lead to an increase in yield. This finding is consistent with the pareto chart results presented in Fig. 1 and the discussion in the previous paragraph. While the negative coefficients of solvent composition (X_2) and amplitude (X_3) indicate that increases in these variables may lead to a decrease in yield under the tested conditions.

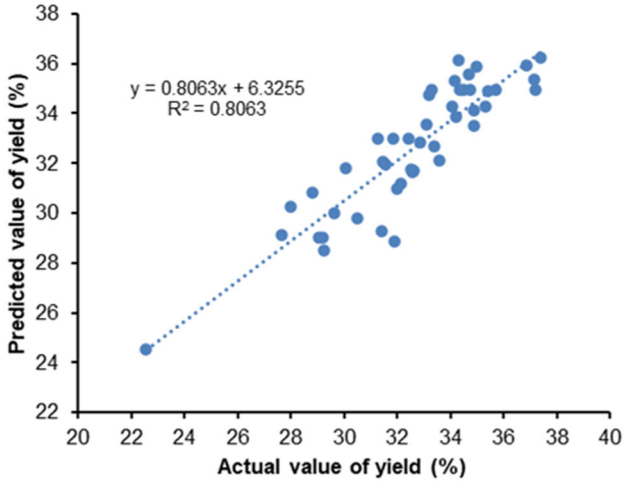

Fig 2. Regression obtained using the actual value of %yield (X axis) and predicted value of %yield from the model (Y axis)

Table 3. ANOVA for the quadratic model adjusted to the PFO yield

Variables	Factors	Coefficients	Sum of squares	Degrees of freedom	Mean square	F-ratio	*p*-value
Temperature	X_1	0.63	6.50	1	6.50	2.24	0.1471
Solvent composition	X_2	2.18	76.21	1	76.21	26.23	0.0000
Amplitude	X_3	2.47	98.15	1	98.15	33.78	0.0000
Solvent to sample ratio	X_4	1.25	25.07	1	25.07	8.63	0.0070
Cycle	X_5	0.00	0.00	1	0.00	0.00	0.9943
Temperature × temperature	X_1X_1	−1.47	18.89	1	18.89	6.50	0.0173
Temperature × solvent composition	X_1X_2	−0.84	2.83	1	2.83	0.97	0.3331
Temperature × amplitude	X_1X_3	1.12	5.02	1	5.02	1.73	0.2007
Temperature × solvent to sample ratio	X_1X_4	1.11	4.95	1	4.95	1.70	0.2039
Temperature × cycle	X_1X_5	0.64	1.66	1	1.66	0.57	0.4562
Solvent composition × solvent composition	X_2X_2	−2.22	43.03	1	43.03	14.81	0.0007
Solvent composition × amplitude	X_2X_3	2.04	16.75	1	16.75	5.76	0.0241
Solvent Composition × solvent to sample ratio	X_2X_4	−0.61	1.53	1	1.53	0.53	0.4745
Solvent Composition × cycle	X_2X_5	−0.91	3.31	1	3.31	1.14	0.2958
Amplitude × amplitude	X_3X_3	−1.49	19.51	1	19.51	6.72	0.0157
Amplitude × solvent to sample ratio	X_3X_4	0.33	0.45	1	0.45	0.16	0.6964
Amplitude × cycle	X_3X_5	0.69	1.93	1	1.93	0.66	0.4225
Solvent to sample ratio × solvent to sample ratio	X_4X_4	−0.90	7.12	1	7.12	2.45	0.1299
Solvent to sample ratio × cycle	X_4X_5	0.54	1.19	1	1.19	0.41	0.5277
Cycle × cycle	X_5X_5	0.49	2.10	1	2.10	0.72	0.4036
Total error			72.63	25	2.91		
Total (corr.)			375.06	45			

$$\begin{aligned}\text{Yield }(\%) = {} & 34.9522 + 0.637544 * X_1 - 2.18246X_2 - 2.47672X_3 \\ & + 1.25184X_4 + 0.00309375X_5 - 1.47103X_1^2 - 0.841125X_1X_2 \\ & + 1.12005X_1X_3 + 1.112X_1X_4 + 0.64505X_1X_5 - 2.22047X_2^2 \\ & - 2.04615X_2X_3 - 0.6188X_2X_4 - 0.91X_2X_5 - 1.49533X_3^2 \\ & + 0.33645X_3X_4 + 0.69495X_3X_5 - 0.903525X_4^2 + 0.545875X_4X_5 \\ & - 0.490158X_5^2\end{aligned} \quad (4)$$

A lack-of-fit test is the variation of the data around the fitted model. It was carried out in order to ascertain whether the selected model was satisfactory to describe the observed data or whether a more complex model is required. The test was performed by comparing the variability of the current model residuals to the variability between observations at replicate settings for the factors. A nonsignificant lack of fit ($p > 0.05$) is a desirable statistical parameter that proves the model fits the responses [25]. Since the *p*-value for the lack-of-fit (0.20) obtained by ANOVA is greater than 0.05, the model appears to be satisfactory for the observed data at the 95.0% confidence level. The correlation coefficients (R^2) represent the confidence that the regression equations would predict the observed value better than the mean [26]. The R^2 statistic indicates that the model as fitted explains 80.63% of the variability in the extraction yield. The standard error of the predicted value shows that the standard deviation of the residuals is 1.33469. Therefore, the model can be used to estimate the response for optimization purposes.

Response Optimization

Significant independent factors are essential to achieve the best extraction yield when optimizing the method. On the basis of the predicted model, three-dimensional surface plots were constructed to predict the relationships between independent factors and the response. The DOE results enabled the construction of the surface response and the variables temperature (X_1) and solvent composition (X_2) were evaluated and the amplitude (X_3), solvent to sample ratio (X_4), and cycle (X_5) were in the center point, as shown in Fig. 3. A high point was found at which the optimum yield (38.40%) was obtained at coordinates for the temperature (X_1) of 0.937814, the solvent composition (X_2) of −0.593737, amplitude (X_3) of −0.64787, solvent to sample ratio (X_4) of 0.99999, and the cycle (X_5) of 1. Based on RSM, the optimum condition for the extraction of PFO using UAE was achieved by extraction temperature of 59 °C, a solvent composition of 42%. an amplitude of 41%, a solvent to sample ratio of 20:1, and a cycle of 0.8.

Extraction Kinetics

Once the effects of the variables on the extraction methods and the optimal values were known, the kinetics of the extractions were further studied. Several extraction experiments were carried out under optimal ultrasound conditions while the extraction time varied between 5, 10, 15, 20, 25, 30, and 35 min. The results of this particular study are shown in Fig. 4. The result of the kinetic study showed that the highest extraction yield for

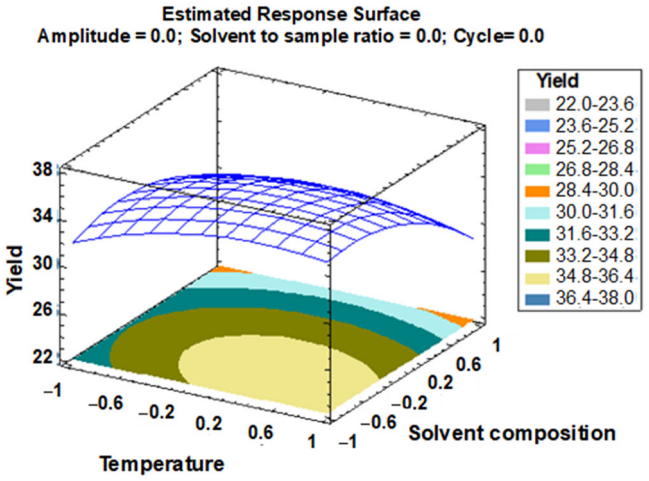

Fig 3. Response surface plot showing effect of variables to the yield

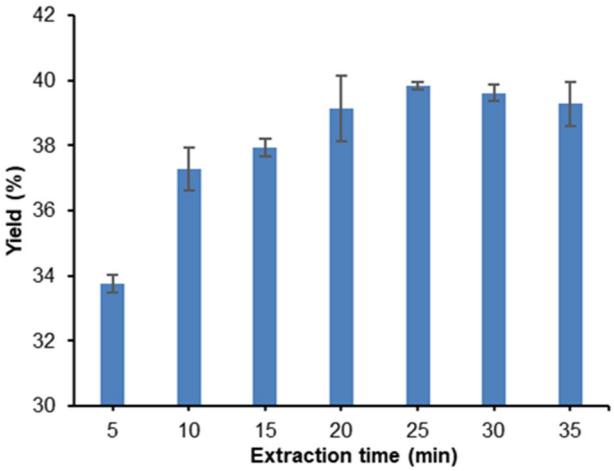

Fig 4. Effect of the extraction time on the PFO yield

PFO using UAE was obtained after 25 min of extraction. After the extraction of 25 min, the PFO extraction yield is decreased. A similar trend was reported by Biswas et al. [14]. In some experiments that use UAE as an extraction method, the extraction yield was significantly time-dependent and increased with extended ultrasonic times, especially from 2 to 20 min, but then slowly from 20 to 40 min. While Zhang et al. [16] also reported that the effect of ultrasound is effective in the first 30 min. However, longer extraction times led to lower yield, probably due to degradation of the oil. So, a 25 min was chosen as the optimum extraction time.

Method Validation

The precision of the method was evaluated for method validation. The precision was determined by performing repeatability (intra-day) and intermediate precision (extra-day) experiments. Repeatability was assessed by 9 independent analyses of the same samples on the same day, while intermediate precision was determined by three independent analyses on three consecutive days. Both precision indicators are expressed as a coefficient of variance (CV) with reference to the yield of PFO. The acceptable CV limit is ±10%, according to the AOAC manual for the Peer-Verified Methods program [27]. The CV values for precision and repeatability were 2.79 and 1.21%, respectively, confirming that the method has a high precision.

Fatty Acids Composition

Since the importance of omega-3 and omega-6 fatty acids as dietary supplements, which have many benefits for human health, it is necessary to know the fatty acid content in the PFO. The fatty acid profile of PFO was analyzed using GC-MS and categorized into saturated fatty acids (SFA), monounsaturated fatty acids (MUFA), and polyunsaturated fatty acids (PUFA). The results (Table 4) are expressed as a percentage of the total fatty acid content (mean ± SD). Among the saturated fatty acids, stearic acid (C18:0) was the most abundant, comprising 16.36 ± 0.08%, followed by myristic acid (C14:0) at 9.27 ± 0.04%. Small quantities of saturated fatty acids were found in lauric acid (C12:0), pentadecanoic acid (C15:0), heptadecanoic acid (C17:0), and 18-methyl-nonadecanoic acid (C19:0), with concentrations ranging from 0.24 to 0.52%. Oleic acid (C18:1) made up 40.73 ± 0.28% of the MUFA group, followed by palmitoleic acid (C16:1) at 3.49 ± 0.07% and vaccenic acid (C18:1n7) at 2.46 ± 0.05%. There were smaller amounts of other MUFAs, such as cis-10-heptadecenoic acid (C17:1) and cis-11-eicosenoic acid (C20:1), which measured 0.23 ± 0.01% and 1.63 ± 0.03%, respectively.

Table 4. Fatty acid composition of PFO

Fatty acid of PFO	Structure	%
Saturated fatty acid		
Lauric acid	C12:0	0.38 ± 0.01
Myristic acid	C14:0	9.27 ± 0.04
Pentadecanoic acid	C15:0	0.50 ± 0.00
Heptadecanoic acid	C17:0	0.52 ± 0.00
Stearic acid	C18:0	16.36 ± 0.08
18-Methyl-nonadecanoic acid	C19:0	0.24 ± 0.00
Monounsaturated fatty acid		
Palmitoleic acid	C16:1	3.49 ± 0.07
cis-10-Heptadecanoic acid	C17:1	0.23 ± 0.01
Oleic acid	C18:1	40.73 ± 0.28
Vaccenic acid	C18:1n7	2.46 ± 0.05
cis-11-Eicosanoic acid	C20:1	1.63 ± 0.03
Polyunsaturated fatty acid		
Linoleic acid	C18:2n6	19.06 ± 0.04
γ-linolenic acid	C18:3n6	0.38 ± 0.01
α-linolenic acid	C18:3n3	1.36 ± 0.02
8.11-Eicosadienoic acid	C20:2	0.60 ± 0.02
cis-11.14-Eicosadienoic acid	C20:2	0.21 ± 0.01
cis-5.8.11-Eicosatrienoic acid	C20:3	1.28 ± 0.03
Arachidonic acid	C20:4n-6	0.85 ± 0.02
Eicosapentaenoic acid	C20:5n-3	0.46 ± 0.02

The PUFA content was mainly represented by linoleic acid (C18:2n6) at 19.06 ± 0.04%, followed by α-linolenic acid (C18:3n3) at 1.36 ± 0.02%, and cis-5,8,11-eicosatrienoic acid (C20:3) at 1.28 ± 0.03%. The amount of linoleate acid was higher than that of other fatty acids. Another researcher also found this trend in other Pangasius species [1]. Other notable PUFAs included arachidonic acid (C20:4n-6), eicosapentaenoic acid (EPA, C20:5n-3), γ-linolenic acid (C18:3n6), cis-11,14-eicosadienoic acid (C20:2), and 8,11-eicosadienoic acid (C20:2), with contents ranging from 0.21 to 0.85%. These findings indicate that PFO contains a high

proportion of unsaturated fatty acids, particularly oleic and linoleic acids, which are known for their beneficial effects on human health.

■ CONCLUSION

The ultrasound-assisted extraction (UAE) method developed in this study for extracting patin fish oil (PFO) was successfully optimized using the Box–Behnken design (BBD) in combination with response surface methodology (RSM). The optimal conditions for extraction were identified at a temperature of 59 °C, solvent composition of 42%, amplitude of 41%, a solvent to sample ratio of 20:1, a cycle duration of 0.8, and an extraction time of 25 min. Fatty acid analysis indicated that the PFO extracted via UAE contained omega-3 fatty acids, including α-linolenic acid (ALA) at 1.36% and eicosapentaenoic acid (EPA) at 0.46%, along with omega-6 fatty acids, such as linoleic acid (LA) at 19.06% and arachidonic acid (AA) at 0.85%. The extraction method has been validated, demonstrating acceptable precision and reliability. These results highlight that the UAE technique developed in this study is a cost-effective, simple, and efficient approach for extracting high-quality PFO.

■ ACKNOWLEDGMENTS

The authors extend their gratitude to the Ministry of Research, Technology, and Higher Education of the Republic of Indonesia for their support through the Enhancing International Publication Quality Program (PKPI Sandwich-Like). Appreciation is also given to the University of Cadiz for providing laboratory support.

■ CONFLICT OF INTEREST

The author declares that there is no conflict of interest.

■ AUTHOR CONTRIBUTIONS

Anggita Rosiana Putri, Widiastuti Setyaningsih, and Miguel Palma conceived and design the experiments, Anggita Rosiana Putri and Ceferino Carrera Fernandez conducted the experiments. Abdul Rohman, Widiastuti Setyaningsih, Miguel Palma, Sugeng Riyanto, and Young Pyo Jang supervised the study. Anggita Rosiana Putri, Widiastuti Setyaningsih, and Young Pyo Jang wrote the manuscript. All authors approved to the final version of this manuscript.

■ REFERENCES

[1] Hashim, R.B., Jamil, E.F., Zulkipli, F.H., and Mohd Daud, J., 2015, Fatty acid compositions of silver catfish, *Pangasius* sp. farmed in several rivers of Pahang, Malaysia, *J. Oleo Sci.*, 64 (2), 205–209.

[2] Jia, Y., Huang, Y., Wang, H., and Jiang, H., 2022, A dose-response meta-analysis of the association between the maternal omega-3 long-chain polyunsaturated fatty acids supplement and risk of asthma/wheeze in offspring, *BMC Pediatr.*, 22 (1), 422.

[3] Bowen, K.J., Harris, W.S., and Kris-Etherton, P.M., 2016, Omega-3 fatty acids and cardiovascular disease: Are there benefits?, *Curr. Treat. Options Cardiovasc. Med.*, 18 (11), 69.

[4] Damaiyanti, D.W., Tsai, Z.Y., Masbuchin, A.N., Huang, C.Y., and Liu, P.Y., 2023, Interplay between fish oil, obesity and cardiometabolic diabetes, *J. Formosan Med. Assoc.*, 122 (7), 528–539.

[5] Gutte, K.B., Sahoo, A.K., and Ranveer, R.C., 2015, Effect of ultrasonic treatment on extraction and fatty acid profile of flaxseed oil, *OCL*, 22 (6), D606.

[6] Sallet, D., Souza, P.O., Fischer, L.T., Ugalde, G., Zabot, G.L., Mazutti, M.A., and Kuhn, R.C., 2019, Ultrasound-assisted extraction of lipids from *Mortierella isabellina*, *J. Food Eng.*, 242, 1–7.

[7] Sicaire, A.G., Vian, M.A., Fine, F., Carré, P., Tostain, S., and Chemat, F., 2016, Ultrasound induced green solvent extraction of oil from oleaginous seeds, *Ultrason. Sonochem.*, 31, 319–329.

[8] Chemat, F., Rombaut, N., Sicaire, A.G., Meullemiestre, A., Fabiano-Tixier, A.S., and Abert-Vian, M., 2017, Ultrasound assisted extraction of food and natural products: Mechanisms, techniques, combinations, protocols, and applications – A review, *Ultrason. Sonochem.*, 34, 540–560.

[9] Kumar, K., Srivastav, S., and Sharanagat, V.S., 2021, Ultrasound assisted extraction (UAE) of bioactive compounds from fruit and vegetable processing by-products: A review, *Ultrason. Sonochem.*, 70, 105325.

[10] Tan, C.X., Gun Hean, C., Hamzah, H., and Ghazali, H.M., 2018, Optimization of ultrasound-assisted aqueous extraction to produce virgin avocado oil with low free fatty acids, *J. Food Process Eng.*, 41 (2), e12656.

[11] Setyaningsih, W., Duros, E., Palma, M., and Barroso, C.G., 2016, Optimization of the ultrasound-assisted extraction of melatonin from red rice (*Oryza sativa*) grains through a response surface methodology, *Appl. Acoust.*, 103, 129–135.

[12] González de Peredo, A.V., Vázquez-Espinosa, M., Espada-Bellido, E., Ferreiro-González, M., Amores-Arrocha, A., Palma, M., Barbero, G.F., and Jiménez-Cantizano, A., 2019, Alternative ultrasound-assisted method for the extraction of the bioactive compounds present in myrtle (*Myrtus communis* L.), *Molecules*, 24 (5), 882.

[13] Rohman, A., and Che Man, Y.B., 2011, Palm oil analysis in adulterated sesame oil using chromatography and FTIR spectroscopy, *Eur. J. Lipid Sci. Technol.*, 113 (4), 522–527.

[14] Biswas, A., Dey, S., Xiao, A., Deng, Y., Birhanie, Z.M., Roy, R., Akhter, D., Liu, L., and Li, D., 2023, Ultrasound-assisted extraction (UAE) of antioxidant phenolics from *Corchorus olitorius* leaves: A response surface optimization, *Chem. Biol. Technol. Agric.*, 10 (1), 64.

[15] Jalili, F., Jafari, S.M., Emam-Djomeh, Z., Malekjani, N., and Farzaneh, V., 2018, Optimization of ultrasound-assisted extraction of oil from canola seeds with the use of response surface methodology, *Food Anal. Methods*, 11 (2), 598–612.

[16] Zhang, Z.S., Wang, L.J., Li, D., Jiao, S.S., Chen, X.D., and Mao, Z.H., 2008, Ultrasound-assisted extraction of oil from flaxseed, *Sep. Purif. Technol.*, 62 (1), 192–198.

[17] Mohammadpour, H., Sadrameli, S.M., Eslami, F., and Asoodeh, A., 2019, Optimization of ultrasound-assisted extraction of *Moringa peregrina* oil with response surface methodology and comparison with Soxhlet method, *Ind. Crops Prod.*, 131, 106–116.

[18] Li, H., Pordesimo, L., and Weiss, J., 2004, High intensity ultrasound-assisted extraction of oil from soybeans, *Food Res. Int.*, 37 (7), 731–738.

[19] Sun, X., Jin, Z., Yang, L., Hao, J., Zu, Y., Wang, W., and Liu, W., 2013, Ultrasonic-assisted extraction of procyanidins using ionic liquid solution from *Larix gmelinii* bark, *J. Chem.*, 2013 (1), 541037.

[20] Herrera, M.C., and Luque de Castro, M.D., 2005, Ultrasound-assisted extraction of phenolic compounds from strawberries prior to liquid chromatographic separation and photodiode array ultraviolet detection, *J. Chromatogr. A*, 1100 (1), 1–7.

[21] Machado, A.P.D.F., Pereira, A.L.D., Barbero, G.F., and Martínez, J., 2017, Recovery of anthocyanins from residues of *Rubus fruticosus*, *Vaccinium myrtillus* and *Eugenia brasiliensis* by ultrasound assisted extraction, pressurized liquid extraction and their combination, *Food Chem.*, 231, 1–10.

[22] Purohit, A.J., and Gogate, P.R., 2015, Ultrasound-assisted extraction of β-carotene from waste carrot residue: Effect of operating parameters and type of ultrasonic irradiation, *Sep. Sci. Technol.*, 50 (10), 1507–1517.

[23] Ganguly, M., Debraj, D., Mazumder, N., Carpenter, J., Manickam, S., and Pandit, A.B., 2024, Impact of ultrasonication on the oxidative stability of oil-in-water nanoemulsions: investigations into kinetics and strategies to control lipid oxidation, *Ind. Eng. Chem. Res.*, 63 (23), 10212–10225.

[24] Pingret, D., Fabiano-Tixier, A.S., and Chemat, F., 2014, An improved ultrasound clevenger for extraction of essential oils, *Food Anal. Method*s, 7 (1), 9–12.

[25] Nam, S.N., Cho, H., Han, J., Her, N., and Yoon, J., 2018, Photocatalytic degradation of acesulfame K: Optimization using the Box–Behnken design (BBD), *Process Saf. Environ. Prot.*, 113, 10–21.

[26] Tak, J.W., Gupta, B., Thapa, R.K., Woo, K.B., Kim, S.Y., Go, T.G., Choi, Y., Choi, J.Y., Jeong, J.H., Choi, H.G., Yong, C.S., and Kim, J.O., 2017, Preparation and optimization of immediate release/sustained release bilayered tablets of loxoprofen using Box–Behnken design, *AAPS PharmSciTech*, 18 (4), 1125–1134.

[27] AOAC International, 1998, *AOAC Peer-verified Methods Program: Manual on Policies and Procedures*, Association of Official Analytical Chemists, Rockville, MD, US.